

Acoustic solitary waves in dusty and/or multi-ion plasmas with cold, adiabatic, and hot constituents

Frank Verheest,^{1,2} Manfred A. Hellberg,² and Ioannis Kourakis³

¹*Sterrenkundig Observatorium, Universiteit Gent, Krijgslaan 281, B-9000 Gent, Belgium*

²*School of Physics, University of KwaZulu-Natal, Private Bag X54001, Durban 4000, South Africa*

³*Centre for Plasma Physics, Department of Physics and Astronomy, Queen's University Belfast, BT7 1NN Northern Ireland, United Kingdom*

(Received 29 August 2008; accepted 24 October 2008; published online 25 November 2008)

Large nonlinear acoustic waves are discussed in a four-component plasma, made up of two superhot isothermal species, and two species with lower thermal velocities, being, respectively, adiabatic and cold. First a model is considered in which the isothermal species are electrons and ions, while the cooler species are positive and/or negative dust. Using a Sagdeev pseudopotential formalism, large dust-acoustic structures have been studied in a systematic way, to delimit the compositional parameter space in which they can be found, without restrictions on the charges and masses of the dust species and their charge signs. Solitary waves can only occur for nonlinear structure velocities smaller than the adiabatic dust thermal velocity, leading to a novel dust-acoustic-like mode based on the interplay between the two dust species. If the cold and adiabatic dust are oppositely charged, only solitary waves exist, having the polarity of the cold dust, their parameter range being limited by infinite compression of the cold dust. However, when the charges of the cold and adiabatic species have the same sign, solitary structures are limited for increasing Mach numbers successively by infinite cold dust compression, by encountering the adiabatic dust sonic point, and by the occurrence of double layers. The latter have, for smaller Mach numbers, the same polarity as the charged dust, but switch at the high Mach number end to the opposite polarity. Typical Sagdeev pseudopotentials and solitary wave profiles have been presented. Finally, the analysis has nowhere used the assumption that the dust would be much more massive than the ions and hence, one or both dust species can easily be replaced by positive and/or negative ions and the conclusions will apply to that plasma model equally well. This would cover a number of different scenarios, such as, for example, very hot electrons and ions, together with a mix of adiabatic ions and dust (of either polarity) or a very hot electron-positron mix, together with a two-ion mix or together with adiabatic ions and cold dust (both of either charge sign), to name but some of the possible plasma compositions. © 2008 American Institute of Physics. [DOI: 10.1063/1.3026716]

I. INTRODUCTION

That plasma physics is inherently nonlinear has been shown by observations of electrostatic spikes by experiments onboard satellites, as have laboratory experiments. Such large amplitudes have called for a fully nonlinear description, which has led, in particular for electrostatic solitary waves, to many successful applications of the Sagdeev pseudopotential¹⁻⁵ or of the more recent, equivalent fluid-dynamic paradigm.⁶⁻¹² The preferred analysis has been in terms of solitary waves which propagate with unchanging shape; e.g., as localized hump or dip profiles. In a co-moving frame, the nonlinear structures are stationary ($\partial/\partial t=0$) and localized ($a \rightarrow a_0$ when $x \rightarrow -\infty$), if the propagation is one-dimensional. Here, x and t refer to (one-dimensional) space and time, respectively, and a stands for any of the relevant dependent variables.

In recent years, attention has turned to dusty plasmas, where, besides the traditional electrons and ions, one also encounters heavier charged dust grains of different kinds. These mixtures of usual plasmas (electrons, ions) plus dust grains, charged in plasma and radiative environments, occur in the heliosphere; e.g., in noctilucent clouds (in the Earth's

polar summer mesosphere), in planetary rings (as spokes and braids), and presumably near comet nuclei and tails. Larger dusty plasmas in molecular interstellar clouds could require also self-gravitation to be taken into account. Other applications range from astrophysics to strongly coupled dusty plasmas and dusty plasma crystals to technology (plasma etching and deposition). Further details can be found in review papers and monographs devoted to this challenging subject.¹³⁻¹⁸

In view of the space and time scales associated with the charged dust components, vastly different from those related to the usual ions and electrons, the simplest modeling has treated the charged dust as monodisperse, heavy negative ions, in the presence of hotter electrons and (positive) ions. While in the normal ion-acoustic regime the charged dust can almost be considered as a neutralizing but immobile background, so that the charge imbalance between the electrons and the protons is the main change compared to what happens in normal plasmas, at the lowest end of the frequency spectrum the dust motion has to be taken into account. Here the prime example is the dust-acoustic mode, well studied both in theory^{19,20} and in the laboratory.²¹

The simplest model at this very low frequency end of the spectrum has been to describe the electrons and ions by Boltzmann distributions, and to treat the dust as cold, in view of its great inertia. While this has helped us to obtain a first description of nonlinear dust-acoustic modes, some of these simplifications severely limit the available parameter space for which solitary waves can be found, in a way which is not always immediately transparent. Hence the efforts in the literature to extend the description by trying to include inertial or thermal effects in a more general way, and also to determine the physical reasons behind the limitations in the space of the compositional parameters.

In the commonly used charging model, the dust grains would be essentially charged by the capture of the more mobile electrons, and thus they become negatively charged. Lighter grains, however, might well be charged positively due to, e.g., photoionization, as is assumed to be the case in the outer part of the rings of Saturn. There have also been observations of the coexistence of negative and positive dust in the Earth's magnetosphere, and hence there is a recent interest in dusty plasma models containing both negatively and positively charged dust.^{22–26} However, all these papers either treat both negative and positive dust species as supersonic, viz., as cool measured in terms of the nonlinear structure speed,²⁷ but deal with the dust-acoustic regime, or else are describing the dust-modified ion-acoustic regime.

The model which we originally had in mind was inspired by a multispecies plasma consisting of four species: hot isothermal electrons and ions, cold, negative, heavy dust grains and adiabatic, positive, lighter dust. For solitary waves where the dust dynamics plays a role, the lighter plasma particles can be assumed to be Boltzmann distributed without great loss of accuracy. The heavy (negative) dust would then be treated as cold, neglecting its thermal effects (pressure), while retaining both inertia and pressure for the other (positive) dust, in an adiabatic description which also aids analytical tractability. We can then address the case where the heavier dust is supersonic, in the fluid-dynamic parlance,^{7,9} whereas the lighter dust is subsonic. This will lead to a novel dust-acoustic-like mode, based on an interplay between the two dust species, which will enable us to describe the hot electrons and plasma ions as superhot, as explained below.

However, when doing the analysis it turned out that we could render the description general enough to deal also with multi-ion plasmas, by replacing one or both of the dust constituents by ions, which are cooler than the isothermal hot ions. The reasons for this adaptability are twofold: On the one hand it was not necessary to make use of the large mass-to-charge ratios characteristic of dust to simplify the algebra, so that ordinary ionic species could be dealt with, and on the other hand the dust is treated as (heavy) negative or positive ions with a constant charge; i.e., the effect of dust charging is neglected.

Although the latter description is a simplification, assuming constant grain charge nevertheless remains a good model to bring out the essential characteristics of dusty plasma waves without undue complexity. Dust charging to the ambient plasma potentials is fast on the dust-acoustic timescale, and thus requires instantaneous response from the

electrons and ions when dust charges fluctuate. The use of Boltzmann distributions for the hot species is in contradiction with this, since such distributions imply that the ion and electron mass and momentum densities are conserved and inertial effects are ignored. Fluctuating dust charges necessarily cause sink and/or source terms to appear in the electron and ion governing equations so that, methodologically speaking, Boltzmann distributions are only compatible with constant dust charges.

Because we feel that it would detract from the readability of the paper if we had to say, at every step in our exposition, “dust” or, equivalently, “cold or adiabatic ions,” we have organized the paper in such a way that we use the dusty plasma terminology in Secs. II–IV, as originally intended. Nevertheless, the analytical exposition is kept general and transcends the dusty plasma model, and we would hope that the reader can keep this in mind.

Sections II deals with the basic formalism and the derivation of the Sagdeev pseudopotential to describe large amplitude solitary waves. In Secs. III and IV we treat dust species with different signs (as in the original motivation) and with equal signs, respectively, and see that there are substantial differences in the possibilities for the solitary wave polarities.

Rather than producing many plots of Sagdeev pseudopotentials for which the numerics show that solutions can be found, we have endeavored, based on physical arguments, to circumscribe the regions in parameter space where solitary waves can occur. Once these existence regions are obtained and discussed for dusty plasmas, one or both dust species are replaced by more usual ions in Sec. V. Finally, our conclusions are summed up in Sec. VI.

II. FORMALISM AND SAGDEEV PSEUDOPOTENTIALS

We start from a plasma model containing four species that are stationary in an inertial frame: cold dust/ions, adiabatic dust/ions, hot isothermal ions, and hot isothermal electrons. Because there are quite a number of parameters involved, we use for the time being the original physical quantities, and will only at a later stage decide upon a suitable or practical set of nondimensional variables.

A. Plasma densities

In the absence of inertial effects, the electron and ion densities are given by

$$\begin{aligned} n_e &= n_{e0} \exp\left[\frac{e\phi}{T_e}\right], \\ n_i &= n_{i0} \exp\left[-\frac{e\phi}{T_i}\right], \end{aligned} \quad (1)$$

where n_s and T_s will refer to the number densities and kinetic temperatures, respectively, of species s , with $s=e$ for the electrons and $s=i$ for the singly charged (positive) ions. Furthermore, ϕ is the electrostatic potential.

The cold dust, with subscript $s=c$, has a typical density given by

$$n_c = \frac{n_{c0}}{\sqrt{1 - \frac{2q_c\phi}{m_c V^2}}}, \tag{2}$$

with m_c and q_c the cold dust mass and charge, respectively, and V the velocity of the solitary wave as seen in an inertial frame. However, we will work in the wave frame, and then V corresponds to the undisturbed plasma velocities far away from the solitary wave.

The adiabatic dust density will have contributions coming from both its inertia and its pressure, and we use a fluid description consisting of the continuity equation

$$\frac{\partial n_a}{\partial t} + \frac{\partial}{\partial x}(n_a v_a) = 0, \tag{3}$$

and of Euler's equation of one-dimensional motion,

$$\left(\frac{\partial}{\partial t} + v_a \frac{\partial}{\partial x}\right)v_a + \frac{1}{n_a m_a} \frac{\partial p_a}{\partial x} = -\frac{q_a}{m_a} \frac{\partial \phi}{\partial x}, \tag{4}$$

with m_a , q_a , and p_a the adiabatic dust mass, charge, and scalar pressure, respectively, using the subscript $s=a$. We use the stationary form of the equation of continuity (3) and obtain a first integral expressing mass flux conservation

$$n_a v_a = n_{a0} V. \tag{5}$$

For adiabatic pressure-density relations $p_a \propto n_a^3 \propto v_a^{-3}$, where the latter proportionality holds in view of Eq. (5). After integration, the stationary form of Eq. (4) becomes a biquadratic equation in v_a (or in n_a , depending on which point of view one wishes to take),

$$\frac{1}{2}(v_a^2 - V^2) + \frac{c_{ta}^2}{2} \left(\frac{V^2}{v_a^2} - 1\right) = -\frac{q_a}{m_a} \phi. \tag{6}$$

Using Eq. (5) to rewrite this in terms of densities yields

$$M_a^2 \left(\frac{n_{a0}}{n_a}\right)^2 - \left(1 + M_a^2 - \frac{2q_a\phi}{m_a c_{ta}^2}\right) + \left(\frac{n_a}{n_{a0}}\right)^2 = 0. \tag{7}$$

Here a "Mach number" M_a and thermal velocity c_{ta} are defined by

$$M_a = \frac{V}{c_{ta}} \quad \text{and} \quad c_{ta}^2 = \frac{3p_{a0}}{n_{a0} m_a}. \tag{8}$$

In principle, one can normalize parameters and variables in various ways, but in the superhot approximation, introduced further on, c_{ta} is the only (constant) velocity scale playing an explicit role, and hence we have used it as the yardstick for all velocities, rather than the dust-acoustic velocity which changes whenever the relative dust densities change. The present choice has the advantage of not introducing hidden changes in the discussion we give later on. The general solution of Eq. (7) in terms of n_a^2 is

$$n_a^2 = \frac{n_{a0}^2}{2} \left[1 + M_a^2 - \frac{2q_a\phi}{m_a c_{ta}^2} \pm \sqrt{\left(1 + M_a^2 - \frac{2q_a\phi}{m_a c_{ta}^2}\right)^2 - 4M_a^2} \right], \tag{9}$$

where the + sign has to be used for a subsonic species ($M_a < 1$) and the - sign for a supersonic one ($M_a > 1$), in order that for $\phi=0$, the correct limit n_{a0} is obtained. This reasoning is based on the fact that $\sqrt{(1-M_a^2)^2} = |1-M_a^2| = 1-M_a^2$ for $M_a < 1$, but becomes M_a^2-1 when $M_a > 1$. The same sign convention has been used in the remainder of this section; namely, the upper sign refers to subsonic species ($M_a < 1$) and the lower sign to supersonic ones ($M_a > 1$).

Following the ideas of Ghosh *et al.*,²⁸ we look for solutions n_a in the form

$$n_a = n_{a0}(\sqrt{a} \pm \sqrt{b}). \tag{10}$$

Substitution of Eq. (10) into Eq. (9) with the same sign convention allows us to determine a and b , and to express the densities as

$$n_a = \frac{n_{a0}}{2} \left[\sqrt{(1+M_a)^2 - \frac{2q_a\phi}{m_a c_{ta}^2}} \pm \sqrt{(1-M_a)^2 - \frac{2q_a\phi}{m_a c_{ta}^2}} \right]. \tag{11}$$

Again, the \pm signs refer to subsonic/supersonic species. The advantage of expressing the density in this way is that it allows for a straightforward integration, needed in what follows.

As an aside, if the adiabatic dust behavior, as reflected by the left hand side of Eq. (6), were only governed by pressure, we would put $M_a=0$ in Eq. (7) and obtain

$$n_a = n_{a0} \sqrt{1 - \frac{2q_a\phi}{m_a c_{ta}^2}}. \tag{12}$$

Since the neglect of inertial effects means that the adiabatic dust is subsonic and warm, this expression for the density can also be obtained by using the upper sign in front of the second square root in Eq. (11) and setting $M_a=0$. However, in what follows we will consider the full adiabatic expressions (11).

B. Sagdeev pseudopotentials

Having thus obtained all constituent densities, we introduce their coupling in Poisson's equation,

$$\frac{d^2\phi}{dx^2} + \frac{1}{\epsilon_0}(en_i - en_e + q_c n_c + q_a n_a) = 0. \tag{13}$$

After multiplication by $d\phi/dx$ and integration, one gets

$$\frac{1}{2} \left(\frac{d\phi}{dx}\right)^2 + \mathcal{S}(\phi) = 0. \tag{14}$$

This result looks like an energy integral in classical mechanics for a particle with unit mass in a conservative force field, with ϕ in the role of the particle coordinate and x in the role of time. The potential energy is then $\mathcal{S}(\phi)$, called the Sagdeev potential or pseudopotential.

Using expressions (1), (2), and (11) we compute the explicit form of the Sagdeev pseudopotential:

$$\begin{aligned}
 S(\phi) = & \frac{n_{e0}T_e}{\epsilon_0} \left(1 - \exp\left[\frac{e\phi}{T_e}\right] \right) + \frac{n_{i0}T_i}{\epsilon_0} \left(1 - \exp\left[-\frac{e\phi}{T_i}\right] \right) \\
 & + \frac{n_{c0}m_cV^2}{\epsilon_0} \left(1 - \sqrt{1 - \frac{2q_c\phi}{m_cV^2}} \right) \\
 & + \frac{n_{a0}m_a c_{ta}^2}{6\epsilon_0} \left\{ 2 + 6M_a^2 - \left[(1 + M_a)^2 - \frac{2q_a\phi}{m_a c_{ta}^2} \right]^{3/2} \right. \\
 & \left. \mp \left[(1 - M_a)^2 - \frac{2q_a\phi}{m_a c_{ta}^2} \right]^{3/2} \right\}. \tag{15}
 \end{aligned}$$

Now is the time to introduce dimensionless variables, normalized with respect to the characteristics of the adiabatic species. To begin with, the electrostatic potential is $\varphi = |q_a|\phi/m_a c_{ta}^2$. For the charges, we will separate the sign from the magnitude, so that $q_c = \sigma_c|q_c|$ and $q_a = \sigma_a|q_a|$, with σ_c and σ_a equal to ± 1 . We also need $\mu = m_a|q_c|/m_c|q_a|$, which is the normalized charge-to-mass ratio of the cold dust. For the temperatures of the two Boltzmann species we use $\tau_e = em_a c_{ta}^2/T_e|q_a|$ and $\tau_i = em_a c_{ta}^2/T_i|q_a|$. Finally, there are the dimensionless (charge) densities of the cold dust, $f = n_{c0}|q_c|/n_{a0}|q_a|$, and the ions, $g = en_{i0}/n_{a0}|q_a|$, so that for the electrons we obtain $en_{e0}/n_{a0}|q_a| = g + \sigma_a + \sigma_c f$. For brevity, we will omit the subscript a on M_a and write simply M . We have chosen to normalize with respect to the adiabatic dust, and hence have implicitly assumed that its (undisturbed) density is never zero; i.e., the adiabatic dust (or its ion equivalent) is always present.

In this way, $S(\phi)$ is recast in dimensionless form as

$$\begin{aligned}
 S(\varphi) = & \frac{g + \sigma_a + \sigma_c f}{\tau_e} (1 - \exp[\tau_e \varphi]) + \frac{g}{\tau_i} (1 - \exp[-\tau_i \varphi]) \\
 & + \frac{fM^2}{\mu} \left(1 - \sqrt{1 - \frac{2\sigma_c \mu \varphi}{M^2}} \right) + \frac{1}{6} \{ 2 + 6M^2 \\
 & - [(1 + M)^2 - 2\sigma_a \varphi]^{3/2} \mp [(1 - M)^2 - 2\sigma_a \varphi]^{3/2} \}. \tag{16}
 \end{aligned}$$

If need be, the dimensionless space coordinate is $\xi = \omega_{pa}x/c_{ta}$, where the adiabatic dust plasma frequency ω_{pa} is defined through $\omega_{pa}^2 = n_{a0}q_a^2/\epsilon_0 m_a$. Since the Sagdeev pseudopotentials already have $S(0)=0$ and $(dS/d\varphi)(0)=0$, the ‘‘origin’’ must be unstable for a solitary solution to (14) to exist, the condition for which is, in general,

$$\frac{d^2S}{d\varphi^2}(0) = \frac{f\mu}{M^2} - \frac{1}{1 - M^2} - [(g + \sigma_a + \sigma_c f)\tau_e + g\tau_i] < 0, \tag{17}$$

often called the soliton condition. We recall that the M values determined from $(d^2S/d\varphi^2)(0)=0$ are precisely the Mach numbers corresponding to the global acoustic velocities for the model envisaged. Hence, there are in this model two acoustic Mach numbers, the expressions for which can be approximated by

$$M^2 \simeq 1 + \frac{1 + f\mu}{(g + \sigma_a + \sigma_c f)\tau_e + g\tau_i} > 1, \tag{18}$$

$$M^2 \simeq \frac{f\mu}{1 + f\mu + (g + \sigma_a + \sigma_c f)\tau_e + g\tau_i} < 1.$$

In the first regime the adiabatic dust is supersonic (cool); in the second subsonic (warm).

Last but not least, we will approximate the electrons and ions as superhot, meaning that the limits $\tau_e \rightarrow 0$ and $\tau_i \rightarrow 0$ are taken. This assumption results in a linearization of the electron and ion contributions in $S(\varphi)$, giving from (16) that

$$\begin{aligned}
 S(\varphi) = & -(\sigma_a + \sigma_c f)\varphi + \frac{fM^2}{\mu} \left(1 - \sqrt{1 - \frac{2\sigma_c \mu \varphi}{M^2}} \right) \\
 & + \frac{1}{6} \{ 2 + 6M^2 - [(1 + M)^2 - 2\sigma_a \varphi]^{3/2} \\
 & \mp [(1 - M)^2 - 2\sigma_a \varphi]^{3/2} \}. \tag{19}
 \end{aligned}$$

Interestingly, this expression does not explicitly contain the ion density (g), and the value of g is thus arbitrary, subject to any requirements that may be imposed by the charge equilibrium conditions and by the necessity of having non-negative densities of the three other components. In particular, we may thus apply this formalism to a three-component system in which there are no hot ions, i.e., electrons and two dust species, one cold and one adiabatic, and of which at least one must be positively charged.

In the superhot approximation, the high acoustic regime of Eq. (18) disappears out of reach towards infinity, and in the low acoustic regime, Eq. (18) gives

$$M^2 > M_s^2 := \frac{f\mu}{1 + f\mu}. \tag{20}$$

When multiplied by c_{ta}^2 , this definition of M_s^2 yields the square of the dust-acoustic velocity, and thus the inequality $M^2 > M_s^2$ expresses the condition that the solitary waves be super-acoustic with respect to the true dust-acoustic velocity in the plasma model.

In this low acoustic range the adiabatic dust is subsonic ($M < 1$) and warm, and hence in all relevant expressions the upper signs have to be retained and the lower ones discarded. When needed, we can invert Eq. (20) and write

$$f_s = \frac{M^2}{\mu(1 - M^2)}. \tag{21}$$

Inspection of Eq. (19) indicates already some limitations on the existence range for φ . On the one hand, the cold dust [see expression (2)] becomes infinitely compressed, which occurs for

$$\varphi_{lc} = \frac{\sigma_c M^2}{2\mu}. \tag{22}$$

On the other hand, the adiabatic dust density [see expression (11)] ceases to be real beyond

$$\varphi_{la} = \frac{\sigma_a}{2}(1-M)^2. \quad (23)$$

This limit corresponds to the adiabatic dust flow hitting a sonic point, where $v_a/V = M_a^{1/2}$ and the local flow speed equals the local thermal velocity, if we briefly return to the original dimensional units. Keeping in mind that in this sonic point Eq. (5) gives $n_a/n_{a0} = M_a^{1/2}$, we find from Eq. (7) that the sonic point occurs when $2q_a\phi/m_a c_{ta}^2 = (1-M_a)^2$, or precisely Eq. (23) in dimensionless variables.

Thus, in order to have solitary waves limited by infinite dust compression, we will need $S(\varphi_{lc}) > 0$ and $S(\varphi_{la}) > 0$. Seeing that Eq. (20) gives a minimum Mach number M_s , the equalities $S(\varphi_{lc}) = 0$ and $S(\varphi_{la}) = 0$ will give the maximum allowable Mach numbers, but we have to specify the model further to see whether these limitations occur on the same or on opposite sides for the potentials.

In addition, the model limit $M < 1$ may not be breached. Moreover, we are working in a fluid description and therefore need to have negligible Landau damping, which means avoiding the thermal speeds of all species. In our case, this implies that M should not be too close to 1, and we could use $M \leq 0.8$ as an indicative guideline, leading consequently to $f\mu \leq 1.75$. These restrictions have to be kept in mind when interpreting some of the existence ranges illustrated in the figures in Secs. III and IV.

III. OPPOSITELY CHARGED COLD AND ADIABATIC DUST COMPONENTS

We now start the discussion of the main model we have in mind, viz. negative cold and positive warm dust. As we shall see, however, the discussion that follows applies equally well to the “reverse case”; i.e., positive cold and negative warm dust. So as to remain general, we shall simply choose $\sigma_a = -\sigma_c$. Hence, φ_{lc} will limit the potential range on the negative or the positive side, depending on the sign of σ_c , and φ_{la} will limit the potential range on the opposite side. Furthermore, the value of μ is arbitrary; i.e., the analysis is not restricted by the choice of the ratio of the charge-to-mass ratios of the two species.

A. Solitary waves limited by infinite cold dust compression

In principle, we have to solve $S(\varphi_{lc}) = 0$ for the maximum Mach numbers as a function of f , but in view of the intricacy of the intervening expressions, we will do this the other way around and solve for the cold dust cutoff values of f as a function of M . This yields

$$f_c = \frac{\mu}{3M^2} \left\{ \left[\left((1+M)^2 + \frac{M^2}{\mu} \right)^{3/2} - 2 - 6M^2 \right] + \left[\left((1-M)^2 + \frac{M^2}{\mu} \right)^{3/2} \right] \right\} - 1. \quad (24)$$

This limiting expression is independent of σ_c and is thus

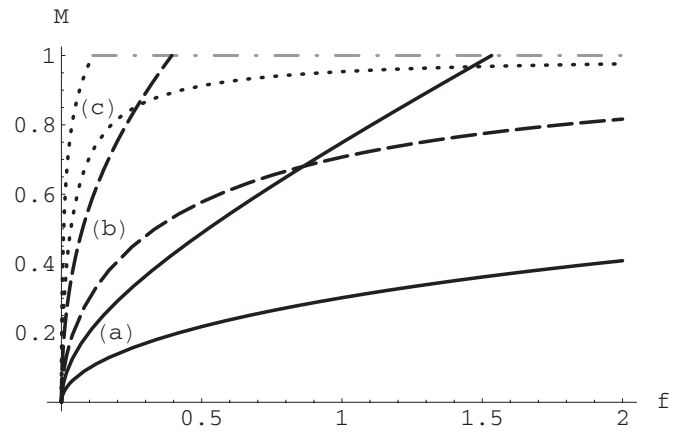


FIG. 1. In each pair of curves, the lower ones express the minimum (soliton) condition, f_s or M_s , the upper ones the occurrence of infinite cold dust compression f_c , the latter for $M < 1$. The gray dot-dashed line indicates the subsonic limit condition $M = 1$. For a given f , the admissible M lie between the upper and the lower curves. The parameter distinguishing the pairs of curves is (a) $\mu = 0.1$ (—), (b) $\mu = 1$ (---), and (c) $\mu = 10$ (···), respectively.

independent of the sign of the cold dust charge. The only thing which changes with σ_c is the polarity of the solitary waves [see Eq. (22)].

One can show that $f_c \rightarrow 0$ for $M \rightarrow 0$, that $f_c > 0$ for all $0 < M < 1$ and that $f_c \rightarrow \infty$ for $M \rightarrow 1$, always for all μ . Even though no analytical difficulties crop up at the extreme values of zero and infinity for f_c , and of zero and 1 for M , these values are not physical because the model breaks down, there being either no cold or warm dust left, or no range for the solitary wave velocities.

We can then plot, for any given value of μ , a pair of curves representing the range [upper/lower bounds, given by Eqs. (20) and (24), respectively] of permitted Mach numbers. We represent three such pairs of curves in Fig. 1, for values of μ equal to 0.1, 1, and 10. These are merely representative of plasma models where the cold dust charge-to-mass ratio is smaller than, equal to, or larger than that of the adiabatic dust, in terms of dust species, as is done in Secs. III and IV. Other values could equally well have been chosen, but values of μ much larger or much smaller would squeeze parts of the plot too much, if shown together in one figure. The choice that we have made clearly indicates what happens if μ increases from smaller to larger, and there are no technical difficulties at all in working with other values for μ .

In each pair of curves, drawn for a given charge-to-mass ratio, the lower one expresses the minimum (soliton) condition, f_s or M_s , the upper one the occurrence of infinite cold dust compression f_c , the latter for $M < 1$. The gray dot-dashed line indicates the subsonic limit condition $M = 1$. For a given f the admissible M lie between the upper and the lower curves. It is seen that the changeover from the infinite cold dust compression limit to $M = 1$ occurs (a) for $\mu = 0.1$ at $f = 1.53$, (b) for $\mu = 1$ at $f = 0.39$, and (c) for $\mu = 10$ at $f = 0.11$. As μ increases, this changeover is encountered for smaller f , but there are no obvious other restrictions on the existence of solitary waves, the polarity of which is determined by the sign of the cold dust charge.

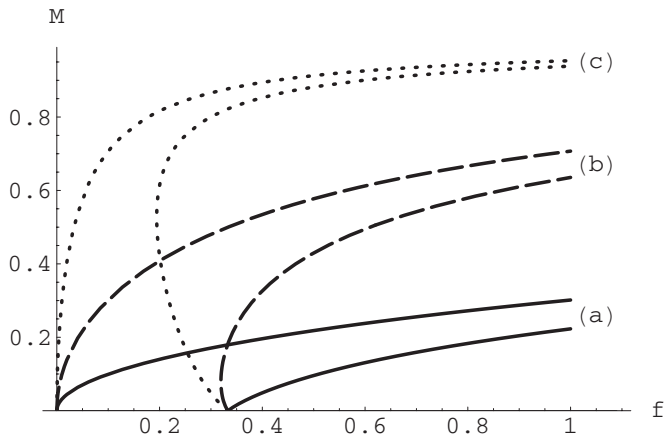


FIG. 2. The curves emanating from $\{f=0, M=0\}$ are the solitary wave conditions (and can be recognized as such in Fig. 1). These should be the “lower” curves. On the other hand, the curves emanating from $\{f=1/3, M=0\}$ represent the condition that the adiabatic dust density is no longer real, and these should be the “upper” curves, lying *above* the lower curves if a proper range in M is to be available. This is clearly not obeyed, so that there can be no solitary waves with an opposite polarity. The parameter distinguishing the pairs of curves is (a) $\mu=0.1$ (—), (b) $\mu=1$ (---), and (c) $\mu=10$ (\cdots), respectively.

B. Solitary waves limited by adiabatic dust density

For solitary waves of the opposite polarity, we have to solve $S(\varphi_{la})=0$, and will follow an analogous procedure, which gives f as a function of M . The expressions are now somewhat more complicated, and we start from

$$S(\varphi_{la}) = Af + B = 0, \tag{25}$$

with A and B defined as

$$A = \frac{M^2}{\mu} \left[1 + \frac{\mu(1-M)^2}{2M^2} - \sqrt{1 + \frac{\mu(1-M)^2}{M^2}} \right], \tag{26}$$

$$B = -\frac{1}{6}(1 - \sqrt{M})^3(1 + 3\sqrt{M}).$$

The behavior of A is such that $A=1/2$ for $M=0$ and $A=0$ for $M \rightarrow 1$, and one can easily show numerically, that for a range of μ from 10^{-4} to 10^4 , A decreases monotonically with M . The other part shows that $B=-1/6$ for $M=0$ and $B=0$ for $M \rightarrow 1$, and B can be proven to be monotonically increasing with M . Hence, we get that

$$f_a = \frac{\mu(1 - \sqrt{M})^3(1 + 3\sqrt{M})}{6M^2 + 3\mu(1 - M)^2 - 6M\sqrt{M^2 + \mu(1 - M)^2}} \tag{27}$$

starts from $1/3$ at $M=0$ and goes to $+\infty$ for $M \rightarrow 1$, if the $0/0$ expression is worked out correctly.

We note already that for $f=1/3$ the solitary wave condition (20) yields $M_s = \mu/(3 + \mu) > 0$. Hence, for this value of f the minimum value for M , namely, M_s , lies above the maximum value $M=0$. This is already a first indication that there will be no solitary waves having a polarity opposite to the one studied in the preceding subsection.

This is borne out by several typical graphs, shown in Fig. 2. The curves emanating from the origin, $\{f=0, M=0\}$,

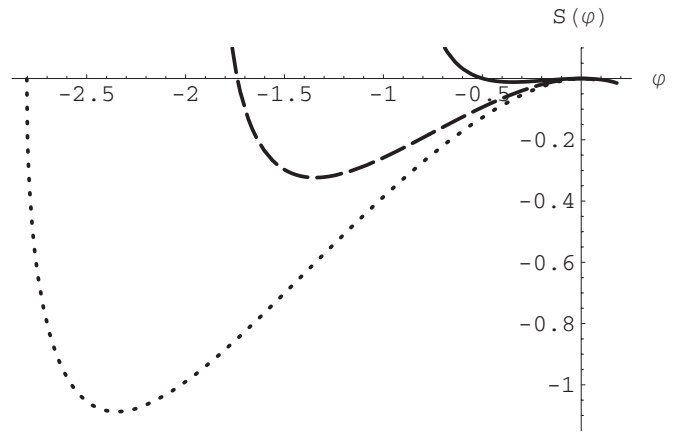


FIG. 3. Sagdeev pseudopotentials for $f=1, \mu=0.1$ and $\sigma_c=-1$. The parameter distinguishing the potentials is $M=0.4$ (—), $M=0.6$ (---), and $M=0.749$ (\cdots), respectively. The latter M value represents the limit on the negative side for which solitary waves can be obtained.

are the solitary wave conditions f_s [cf. Eq. (21)], and can be recognized as such from the corresponding curves in Fig. 1. These should be the “lower” curves. On the other hand, the curves emanating from the point $\{f=1/3, M=0\}$ represent the condition that the adiabatic dust density is no longer real, and these should be the “upper” curves, lying *above* the lower curves, if a proper range in M is to be available. Clearly, this is not obeyed, so that there can be no solitary waves with the opposite polarity.

That this is indeed the case and only solitary waves of the same polarity as the cold dust can exist, is shown by the graphs of typical Sagdeev pseudopotentials in Fig. 3. We have chosen $\sigma_c=-1$ to generate these graphs, but the corresponding ones for $\sigma_c=+1$ are obtained by just inverting the orientation of the φ axis. In principle the graphs are drawn from φ_{lc} to φ_{la} , but for reasons of graphical clarity the range of $S(\varphi) > 0$ has been cut off at 0.1, except for the dotted curve, the end of which lies on the φ axis. For larger M there are no more solutions, as indicated already in Fig. 1. It is obvious from the discussion given in the previous subsection and the resulting limiting curves that many figures such as Fig. 3 can be generated for other values of the compositional parameters f and μ , and for suitable M , as determined from Fig. 1.

Finally, in order to explain in Fig. 2 the curved behavior of the graphs originating in $\{f=1/3, M=0\}$, we note from Eq. (27) that

$$\left. \frac{dM}{df} \right|_{f=1/3} = \frac{3\sqrt{\mu}}{2 - 4\sqrt{\mu}}, \tag{28}$$

and see that the slope changes from positive (for small enough μ) to negative (for larger μ) at $\mu=1/4$. Nevertheless, one can prove that these curves always stays below the f_s curves, although both tend to $M=1$ for $f \rightarrow +\infty$. This is done by examining the ratio

$$r = \frac{f_a}{f_s} = \frac{\mu^2(1 - \sqrt{M})^3(1 + 3\sqrt{M})(1 - M^2)}{3M[2M^3 + \mu M(1 - M)^2 - 2\sqrt{M^2 + \mu(1 - M)^2}]}. \quad (29)$$

As the curves are drawn in Fig. 2, a line drawn parallel to the f axis, for a certain value of M , would first encounter the curve coming from f_s and later the curve representing f_a , and hence these curves never cross, provided $r > 1$. This is indeed the case for all $\mu > 0$, since $r \rightarrow +\infty$ for $M=0$ and $r = 4/3$ when $M \rightarrow 1$. In between, the curve of r shows a minimum lower than $4/3$ but above 1.2 . This has been checked numerically for a wide range of possible μ , and the minimum moves towards the high f side as μ becomes larger.

IV. COLD AND ADIABATIC DUST CHARGES OF THE SAME SIGN

We next turn to the case in which both dust species have the same charge sign, so that now $\sigma_a = \sigma_c$, but we make no assumption about the sign of σ_c . The picture is somewhat different from the earlier discussion in Sec. III. The expression for φ_{lc} is unchanged from Eq. (22), but φ_{la} changes from Eq. (23) to

$$\varphi_{la} = \frac{\sigma_c}{2}(1 - M)^2. \quad (30)$$

Now both limits are on the same side and require a subtler discussion as to their relative positions. The crossover from one limit to the other occurs for

$$M_{co} = \frac{\sqrt{\mu}}{1 + \sqrt{\mu}}, \quad (31)$$

so that for $0 < M < M_{co}$ the infinite cold dust compression is the limiting factor, whereas for $M_{co} < M$ the adiabatic dust density limitation takes over.

It is well known from Sagdeev potential calculations that double layers may represent limiting values for a region in parameter space in which solitary waves may occur.³ Thus, a third possible limitation on the solitary wave amplitude arises from the existence of a double layer, as a limiting case of a set of solitary waves, before one of the sonic points is reached. A double layer is characterized by the coincidence of a zero of the Sagdeev pseudopotential with a zero of its derivative; i.e., with a charge neutral point. This will be investigated in a later subsection dealing with double layers.

For solitary wave potentials with polarity opposite to that associated with φ_{lc} and φ_{la} , we see no obvious physical limitation on φ . By opposite polarity, we mean $\varphi > 0$ for $\sigma_c = \sigma_a = -1$ and $\varphi < 0$ for $\sigma_c = \sigma_a = 1$. However, we note that for this case $S(\varphi)$ is mathematically well behaved for all φ and that $S(\varphi) \rightarrow -\infty$ for $|\varphi| \rightarrow \infty$, as ultimately the terms in $-|\varphi|^{3/2}$ dominate. Combining this information with the required convexity at the origin [Eq. (17)] means that roots for $S(\varphi)$, if they exist on this side at all, must come in pairs, counting possible double roots as two. From the generic behavior we know that a range of possible solitary waves ends when a double layer is encountered.³ Again, Eq. (20) implies the conclusion that the adiabatic dust is subsonic.

A. Solitary waves limited by dust density considerations

Starting now from Eq. (19) with $\sigma_a = \sigma_c$, we solve the two limiting situations $S(\varphi_{lc}) = 0$ and $S(\varphi_{la}) = 0$ for f as functions of M , and get

$$f_c = \frac{\mu}{3M^2} \left\{ \left[(1 + M)^2 - \frac{M^2}{\mu} \right]^{3/2} - 2 - 6M^2 + \left[(1 - M)^2 - \frac{M^2}{\mu} \right]^{3/2} \right\} + 1 \quad (32)$$

and

$$f_a = \frac{\mu(1 - \sqrt{M})^3(1 + 3\sqrt{M})}{6M^2 - 3\mu(1 - M)^2 - 6M\sqrt{M^2 - \mu(1 - M)^2}}, \quad (33)$$

respectively. Comparing Eqs. (32) and (33) to Eqs. (24) and (27), respectively, we note that there are some sign changes, which look slight but will turn out to be significant.

We see that f_c , defined by Eq. (32), only exists for M small enough, so that $0 < M \leq M_{co}$ and indeed, $|\varphi_{lc}| < |\varphi_{la}|$. On the other hand, f_a , defined by Eq. (33), is only meaningful for $M_{co} \leq M$, and now $|\varphi_{la}| < |\varphi_{lc}|$. For $M = M_{co}$ both Eqs. (32) and (33) give the same value,

$$f_{co} = \frac{1}{3}(\sqrt{1 + \sqrt{\mu}} - \sqrt[4]{\mu})^3(\sqrt{1 + \sqrt{\mu}} + 3\sqrt[4]{\mu}). \quad (34)$$

The changeover between cold and adiabatic limits corresponds in $\{f, M\}$ space (a) to $\{0.19, 0.24\}$ for $\mu = 0.1$, (b) to $\{0.11, 0.50\}$ for $\mu = 1$, and (c) to $\{0.04, 0.76\}$ for $\mu = 10$.

Hence, for $0 < M \leq M_{co}$, we follow the curve given by f_c , representing the limit where the cold dust density becomes infinite. For $M_{co} \leq M$, we follow the curve given by f_a , expressing the fact that the adiabatic dust density ceases to be real, until we hit the point where the double layers come in as the limiting factor of the solitary wave amplitudes. As discussed in the next subsection, this occurs (a) at $\{0.66, 0.28\}$ for $\mu = 0.1$, (b) at $\{0.32, 0.55\}$ for $\mu = 1$, and (c) at $\{0.12, 0.79\}$ for $\mu = 10$.

B. Solitary waves limited by double layers

The possible occurrence of double layers signals the end of the Mach number range for solitary waves of a given polarity. Hence the double layer conditions, written in compact form as

$$S(\varphi_m; f, M, \mu) = 0, \quad (35)$$

$$\frac{d}{d\varphi} S(\varphi_m; f, M, \mu) = 0,$$

have been considered for given f and μ . When there is a solution to this problem, one finds the double layer amplitude $|\varphi_m|$ and corresponding M . For larger M , no roots for $S(\varphi)$ are possible on the side considered. This exercise can then be repeated for variable f at fixed μ , in order to generate curves that mimic those found on the side for which the dust density restrictions influence the solitary wave existence domains.

To keep the discussions simple, we will focus in the remainder of this section on the case of two negative dust species, that is $\sigma_c = \sigma_a = -1$, and investigate whether solitary structures can exist for the typical ratios $\mu = 0.1, 1$, and 10 , as used for the other subsections. With $\sigma_c = \sigma_a = +1$, the polarity of the solitary waves and double layers changes, but the existence domains in $\{f, M\}$ space at given μ remain the same.

As we will see, there is a transition from negative to positive double layers. To determine where that will happen, we Taylor expand for weakly nonlinear solitary waves $S(\varphi)$ around the initial condition $\varphi = 0$, which gives

$$S(\varphi) = \frac{1}{2} \left(\frac{f\mu}{M^2} - \frac{1}{1-M^2} \right) \varphi^2 - \left(\frac{f\mu^2}{2M^4} - \frac{1+3M^2}{6(1-M^2)^3} \right) \varphi^3. \tag{36}$$

The coefficient of φ^2 is annulled for $M = M_s$, defined in Eq. (20). In order to obtain a solution, both terms in the expansion must contribute equally, and hence we take $M = M_s + \delta$, with δ of the order of φ . This leads to

$$S(\varphi) = - \frac{(1+f\mu)^{5/2} \delta}{\sqrt{f\mu}} \varphi^2 + \frac{(1+f\mu)^2 (4f^2\mu + f - 3)}{6f} \varphi^3. \tag{37}$$

For small f , both coefficients are negative and hence we will have negative potential solitary waves, whereas for larger f the coefficient of the cubic term turns positive; hence, positive solitary waves are encountered. The change from negative to positive solitary waves occurs at the positive root f_{np} of $4f^2\mu + f - 3 = 0$,

$$f_{np} = \frac{\sqrt{1+48\mu} - 1}{8\mu}. \tag{38}$$

As can clearly be seen from Fig. 4, the changeover point lies in C, where the upper and lower curves touch; hence, M_{np}^2 is determined by inserting f_{np} in Eq. (20), giving

$$M_{np}^2 = \frac{\sqrt{1+48\mu} - 1}{\sqrt{1+48\mu} + 7}. \tag{39}$$

This corresponds (a) to $\{1.76, 0.39\}$ for $\mu = 0.1$, (b) to $\{0.75, 0.66\}$ for $\mu = 1$, and (c) to $\{0.26, 0.85\}$ for $\mu = 10$.

C. Summary

To recapitulate, in this section we have considered two species of negative dust with possibly different charge-to-mass ratios, one being cold, the other adiabatic. On the negative potential side the solitary waves are limited successively, for increasing f , by infinite cold dust compression, by the adiabatic dust sonic point, and by the occurrence of negative double layers, in that order, until the polarity changes at f_{np} . On the positive side, the upper limiting curves consist of two parts, for $M < 1$ the occurrence of positive double layers limits the solitary wave existence domain, until the model limitation $M = 1$ is encountered (a) for $\mu = 0.1$ at $f = 8.64$, (b) for $\mu = 1$ at $f = 2.19$, and (c) for $\mu = 10$ at $f = 0.60$. All these results are shown in Fig. 4. Similarly as was noted from Fig. 1, there are no upper limitations on f here.

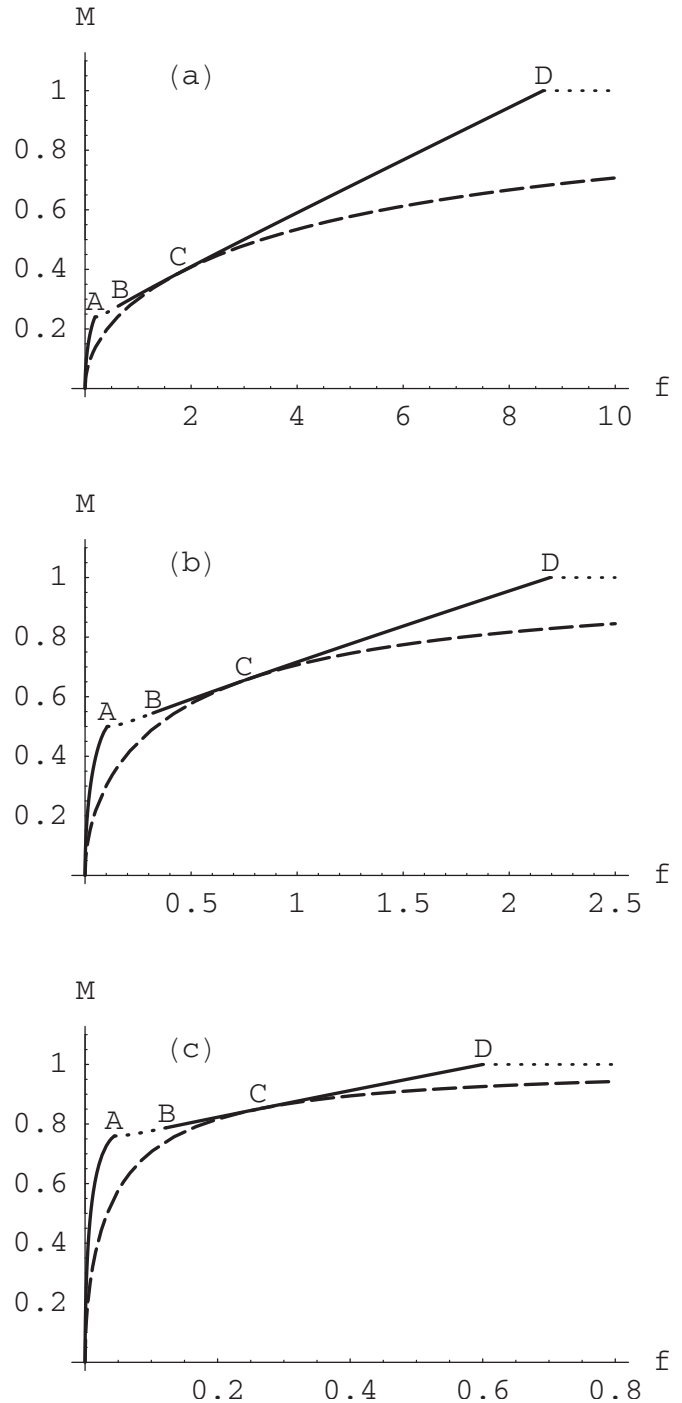


FIG. 4. Existence domains for solitary structures at (a) $\mu = 0.1$, (b) $\mu = 1$, and (c) $\mu = 10$, respectively. In each of the graphs, the upper curves, drawn alternately as full (—) and dotted (···), show the different physical limitations on M as follows: infinite cold dust compression (up to A), adiabatic dust sonic point (AB), double layers (negative on BC and positive on CD), and model restriction $M = 1$ (from D onwards). The lower dashed (---) curve represents the minimum M from the soliton condition.

It is of interest also to know how the maximum solitary wave and double layer amplitudes vary over this parameter space. As an indicative illustration we show in Fig. 5 the behavior of the extreme amplitude φ_m of the solitary wave structures as a function of f for $\mu = 1$; i.e., the case in which the two dust species have not only the same sign of charge, but also the same charge-to-mass ratio. As f increases, φ_m

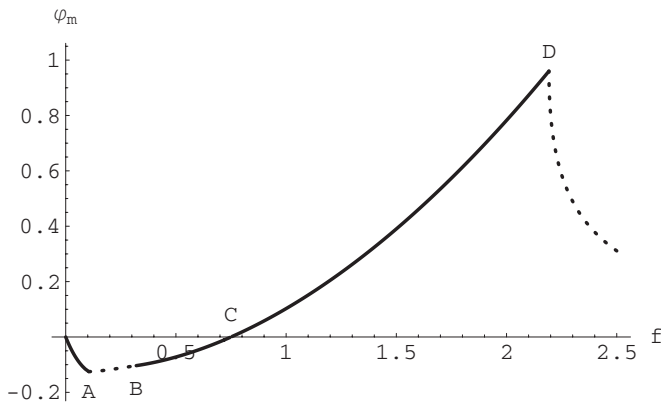


FIG. 5. Extreme amplitudes for solitary structures for $\mu=1$. For the interpretation of the points A, B, C, and D, see Fig. 4.

becomes more and more negative until the point A is reached, where the infinite cold dust compression gives way to the adiabatic dust sonic point limitation. From there on, the amplitudes diminish in absolute value, also when the occurrence of negative double layers takes over at B, until at C we cross from negative to positive double layers. The amplitudes now increase until at D the model restriction $M=1$ comes into play. Thereafter, the maximal amplitudes decrease to zero for $f \rightarrow \infty$. This is illustrated in Fig. 5 for $\mu=1$. Figures for other values of μ , such as 0.1 or 10, are essentially similar, except that the typical magnitudes of the extreme amplitudes φ_m decrease as μ increases and characteristics such as the peak positive and negative amplitudes, as well as the switch of double layer polarity occur at smaller values of f . In order not to overload the paper, these have been omitted.

Further, to check that these limitations are real, we construct typical Sagdeev pseudopotentials, shown in Fig. 6. This figure shows the extreme sensitivity of the double layer criteria, as well as the increase in solitary wave amplitude with M (“taller is faster,” as known from standard Korteweg–de Vries analysis of moderately nonlinear structures, although, as shown in Fig. 7, not “thinner”), until the

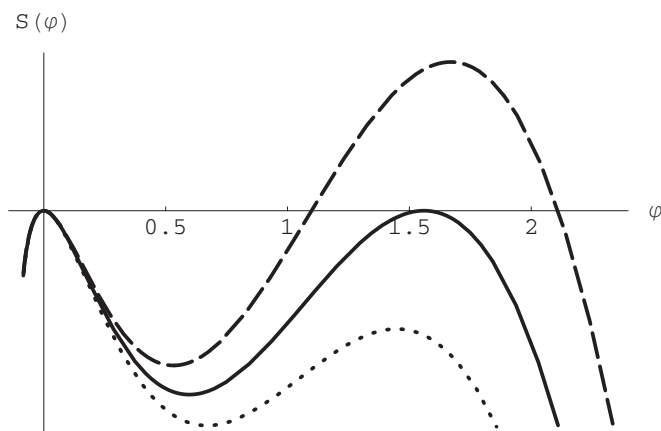


FIG. 6. Sagdeev pseudopotentials for $f=4$ and $\mu=0.1$. The parameter distinguishing the potentials is $M=0.588$ (---, solitary wave), $M=0.590$ (—, double layer), and $M=0.592$ (···, no solutions), respectively.

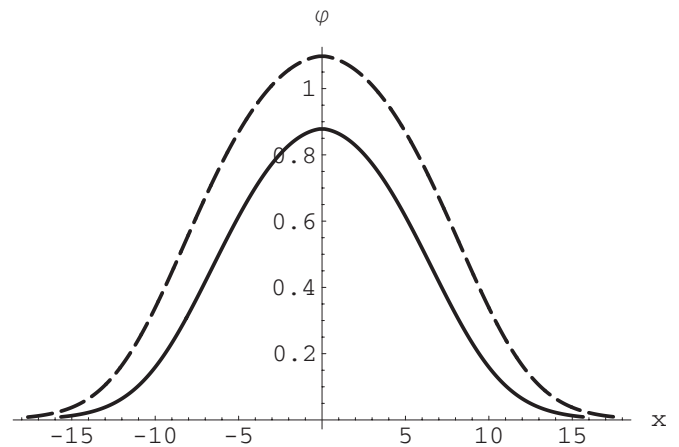


FIG. 7. Typical solitary wave profiles for $f=4$, $\mu=0.1$, and $M=0.585$ (—, lower curve) or $M=0.588$ (---, upper curve). The latter profile gives the solitary wave solution of the dashed Sagdeev pseudopotential pictured in Fig. 6. Taller is indeed faster.

largest structure is found in the double layer, at given f and μ . Countless similar graphs to the ones presented in Fig. 7 can be produced.

We note that when we first started discussing the forming of double layers, we explicitly chose to deal with two negative dust species. However, had we instead chosen the signs of the dust charges to be positive, $\sigma_c = \sigma_a = +1$, we would have found identical $\{f, M\}$ curves, the only difference being the polarity of the solitary structures.

Finally, we have to point out that for $\sigma_c = \sigma_a = -1$ the plasma contains three negative species, and the only positive species is the (Boltzmann) ions, which are superhot; viz., subsonic and inertialess. Nevertheless, we have seen that positive potential solitary structures can be generated in appropriate and acceptable parameter ranges. Similarly, for $\sigma_c = \sigma_a = +1$ the plasma contains three positive species, and the only negative species is the superhot electrons, and yet, negative potential solitary structures can be generated.

This leaves us with the open question of what precisely determines the polarity of the nonlinear waves, and whether this can be figured out or guessed if the composition of the plasma model is given, before doing all the mathematics. From the treatment of many, maybe simpler cases one could be tempted to conclude that one of the cooler, inertial species is driven towards its sonic point and hence the sign of that species fixes the polarity of the nonlinear structures. There are now already several examples where this “rule” has been violated, and so this simple explanation is in general inadequate.

V. MULTI-ION PLASMAS

An important feature of this general analysis is that nowhere have we used the assumption that the dust would be much more massive than the ions. The only mass ratio occurring is $\mu = m_a |q_c| / m_c |q_a|$, and we have taken examples with $\mu < 1$ as well as with $\mu = 1$ or $\mu > 1$. Hence, we can easily replace one or both dust species by positive and/or negative ions and our conclusions will apply to that plasma model equally well.

Furthermore, we noted in Sec. II that the expression for the Sagdeev potential (19) does not contain the ion density explicitly, and thus this work can be applied to the case in which the hot ion density vanishes. Bearing this in mind, we see that the study could be applied equally well to a number of different scenarios; e.g., (a) very hot electrons and ions, together with a mix of adiabatic ions and dust (of either polarity), (b) a very hot electron-positron mix, together with a two-ion mix of either the same or opposite charges, (c) very hot electrons and a two-ion mix (one or both positive), or (d) a very hot electron-positron mix, together with adiabatic ions and cold dust (both of either charge sign).

Previously,¹² we considered a two-ion dusty plasma, composed of superhot electrons, warm and cool ions of the same type (i.e., equivalent to $\mu=1$ in our Sec. IV), and supermassive negative dust. It was shown that in both the superhot and the supermassive approximation, the relevant contribution to the Sagdeev potential could be linearized, and thus they make the same effective contribution. Hence, we see that there are similarities between the earlier work and the present calculation, our superhot ions and electrons replacing the supermassive dust and the superhot electrons.

Further, we found what we termed ion acoustic-like solitary waves,¹² in which the important partners were not the ions and electrons, as is the case for the usual ion acoustic soliton, but the two ion species, and the relevant phase velocity lay between the two ion thermal speeds. We are here again dealing with a phase speed that lies between that of the adiabatic and the cold component and the results of Sec. IV (for instance, Fig. 4), are reminiscent of, but more general than our earlier work.¹²

Moreover, a related scenario was discussed in another earlier work,²⁹ in which electron acoustic solitary waves were considered in a plasma involving immobile ions, cool inertial electrons, and hot electrons whose inertia was not neglected, as is usually the case. Again, the results may be seen to be similar to a three-component model based on that of the type discussed in Sec. IV, with the superhot ions neglected, the superhot electrons replaced by very massive ions, and the two electron species being modelled in a manner similar to our adiabatic and cold components in Sec. IV. The previous results,²⁹ like those found here, showed the maximum Mach number being successively limited by two limiting potentials, followed by double layers, a change of sign of the double layers, and then the restriction imposed by the model, much as we have seen here in Fig. 4.

VI. CONCLUSIONS

We have investigated large nonlinear acoustic waves in a dusty plasma consisting of both cold and adiabatic negative/positive dust, in the presence of superhot isothermal electrons and ions, using a Sagdeev pseudopotential formalism where nonlinear structures are stationary in a co-moving frame. We have delimited the compositional parameter space where large dust-acoustic structures can be found, without restrictions on the charges and masses of the dust species and their charge signs. It was found that in this model the adiabatic dust needs to be subsonic, leading to a novel dust-

acoustic-like mode based on the interplay between the two dust species.

Looking first at oppositely charged cold and adiabatic dust constituents, we find that only solitary waves can exist. These have the polarity of the cold dust, regardless of whether this is negative or positive, and their parameter range is limited by infinite compression of the cold dust. Including adiabatic dust inertia and pressure just modifies the existence regime quantitatively, not qualitatively, compared to earlier studies.

However, when the cold and adiabatic dust charges have the same sign, solitary structures are limited for increasing Mach numbers successively by infinite cold dust compression, by encountering the adiabatic dust sonic point and by the occurrence of double layers. These double layers have, for smaller Mach numbers, the same polarity as the charged dust, but switch at the high Mach number end to the opposite polarity. Typical Sagdeev pseudopotentials and solitary wave profiles have been presented.

Finally, the analysis has nowhere used the assumption that the dust would be much more massive than the ions, so that one or both dust species can easily be replaced by positive and/or negative ions and the conclusions will apply to that plasma model equally well. We have briefly mentioned some of these different scenarios, e.g., very hot electrons and ions, together with a mix of adiabatic ions and dust (of either polarity) or a very hot electron-positron mix, together with a two-ion mix or together with adiabatic ions and cold dust (both of either charge sign), to name a few of the possible plasma compositions, which illustrate the versatility of our approach.

ACKNOWLEDGMENTS

F.V. thanks the Fonds voor Wetenschappelijk Onderzoek (Vlaanderen) and M.A.H. the National Research Foundation for research grants. Any opinion, findings, and conclusions or recommendations expressed in this material are those of the authors and therefore the NRF does not accept any liability in regard thereto. The work of I.K. was supported by a UK EPSRC Science and Innovation Award (at the Centre for Plasma Physics, Queen's University Belfast).

¹R. Z. Sagdeev, in *Reviews of Plasma Physics* Vol. 4, edited by M. A. Leontovich (Consultants Bureau, New York, 1966), pp. 23–91.

²R. Z. Sagdeev and A. A. Galeev, *Nonlinear Plasma Theory* (W.A. Benjamin, New York, 1969).

³S. Baboolal, R. Bharuthram, and M. A. Hellberg, *J. Plasma Phys.* **44**, 1 (1990).

⁴R. Bharuthram and P. K. Shukla, *Planet. Space Sci.* **40**, 973 (1992).

⁵W. K. M. Rice, M. A. Hellberg, R. L. Mace, and S. Baboolal, *Phys. Lett. A* **174**, 416 (1993).

⁶J. F. McKenzie, *Phys. Plasmas* **9**, 800 (2002).

⁷J. F. McKenzie, *J. Plasma Phys.* **67**, 353 (2002).

⁸J. F. McKenzie and T. B. Doyle, *New J. Phys.* **5**, 26 (2003).

⁹F. Verheest, T. Cattaert, G. S. Lakhina, and S. V. Singh, *J. Plasma Phys.* **70**, 237 (2004).

¹⁰J. F. McKenzie, F. Verheest, T. B. Doyle, and M. A. Hellberg, *Phys. Plasmas* **11**, 1762 (2004).

¹¹J. F. McKenzie, F. Verheest, T. B. Doyle, and M. A. Hellberg, *Phys. Plasmas* **12**, 102305 (2005).

¹²M. A. Hellberg, F. Verheest, and T. Cattaert, *J. Phys. A* **39**, 3137 (2006).

¹³D. A. Mendis and M. Rosenberg, *Annu. Rev. Astron. Astrophys.* **32**, 419 (1994).

- ¹⁴M. Horányi, *Annu. Rev. Astron. Astrophys.* **34**, 383 (1996).
- ¹⁵F. Verheest *Space Sci. Rev.* **77**, 267 (1996).
- ¹⁶F. Verheest, *Waves in Dusty Space Plasmas* (Kluwer Academic, Dordrecht, 2000).
- ¹⁷P. K. Shukla and A. A. Mamun, *Introduction to Dusty Plasma Physics* (IOP, London, 2002).
- ¹⁸P. K. Shukla and A. A. Mamun, *New J. Phys.* **5**, 17 (2003).
- ¹⁹N. N. Rao, P. K. Shukla, and M. Y. Yu, *Planet. Space Sci.* **38**, 543 (1990).
- ²⁰F. Verheest, *Planet. Space Sci.* **40**, 1 (1992).
- ²¹A. Barkan, R. L. Merlino, and N. D'Angelo, *Phys. Plasmas* **2**, 3563 (1995).
- ²²P. H. Sakanaka and P. K. Shukla, *Phys. Scr., T* **84**, 181 (2000).
- ²³I. Spasovska and P. H. Sakanaka, *AIP Conf. Proc.* **784**, 506 (2005).
- ²⁴N. Akhtar, S. Mahmood, and H. Saleem, *Phys. Lett. A* **361**, 126 (2007).
- ²⁵A. A. Mamun, *Phys. Lett. A* **372**, 686 (2008).
- ²⁶F. Sayed, M. M. Haider, A. A. Mamun, P. K. Shukla, B. Eliasson, and N. Adhikary, *Phys. Plasmas* **15**, 063701 (2008).
- ²⁷F. Verheest, M. A. Hellberg, and G. S. Lakhina, *Astrophys. Space Sci. Trans.* **3**, 15 (2007).
- ²⁸S. S. Ghosh, K. K. Ghosh, and A. N. Sekar Iyengar, *Phys. Plasmas* **3**, 3939 (1998).
- ²⁹T. Cattaert, F. Verheest, and M. A. Hellberg, *Phys. Plasmas* **12**, 042901 (2005).